

**CYCLIC PLASTICITY BEHAVIOR OF 90° BACK-TO-BACK PIPE BENDS UNDER CYCLIC BENDING AND STEADY PRESSURE**

**Nak-Kyun Cho**

Department of Mechanical & Aerospace  
Engineering, University of Strathclyde  
Glasgow, UK

**Haofeng Chen**

Department of Mechanical & Aerospace  
Engineering, University of Strathclyde  
Glasgow, UK

**ABSTRACT**

Back-to-back pipe bends are widely adopted applications in many industries including nuclear sectors. Evaluation of their load bearing capability under complex cyclic loading is very important. Recently, a couple of research reported shakedown boundary of a 90° back-to-back pipe bends by adopting a conservative approach but no comprehensive post yield structural behaviors have been dealt with. In this research the concerning pipe bends subjected to cyclic opening in-plane (IP)/out-of-plane (OP) bending and steady internal pressures are analyzed to construct shakedown and ratchet limit boundary by means of the Linear Matching Method. Analyzed results present that the concerning pipe bends under out-of-plane bending has higher resistance to cyclic bending than under in-plane bending. In additions, the out-of-plane bending causes very small alternating plasticity areas, unlike the in-plane bending. Full cyclic incremental analyses known as step-by-step analysis are performed to verify the structural responses either side of each boundary and confirm correct responses. Parametric studies are carried out with respect to changes in geometry of the concerning pipe bends subjected to the same loading, and semi-empirical equations are derived from relationships of the reverse plasticity limit and the limit pressure with the bend characteristic. This paper offers comprehensive understandings of structural responses of the 90° back-to-back pipe bends under the complex cyclic loading as well as providing key points to be considered for the life assessment of the piping system.

**INTRODUCTION**

Pipe bends are essential components to efficiently design piping networks for changing direction of the fluid within limited space. To improve the space availability, back-to-back pipe bends formed by bending a straight pipe are widely used on

both small and large scales in the nuclear energy industry. When pipe bends are subjected to the combined cyclic bending and steady pressure, evaluation of their structural behavior is mandatory in order to prevent such increment plastic collapse or crack initiations due to ratchetting or low cycle fatigue (reversed plasticity) respectively. Hence, pipe bends are designed to ensure safety by showing elastic shakedown which allows plastic deformation but causes neither ratchetting nor reversed plasticity.

The shakedown and ratchetting problems are too complex to solve analytically in the general case. Advanced computational analysis such as Incremental Finite Element Analysis or Direct Cyclic Analysis can help predict which structural response (elastic shakedown, reverse plasticity, ratchetting) appears but has limitations on evaluating limit boundary of each structural response, such as Bree diagram [1]. Consequently many direct methods have been developed in basis of Melan[2] and Koiter[3] theorems in order to compute approximate bounds for the shakedown limit loads. Iterative elastic technique is a typical approach which contains Elastic Compensation Method [4], GLOSS R-node method[5], LMM[6], and so on. The LMM has acquired distinguished reputation of providing accurate result for many complicated geometries subjected to complex loading as well as it can consider temperature dependent material parameters[7-9].

Extensive research works have been reported in the literature and experiments on shakedown limit and limit load of a single pipe elbow under the combined cyclic and steady loading[10, 11]. Recently, a couple of works have been published for more complex piping geometries such as ninety degree back-to-back pipe bends[12, 13]. However the published works do not deal with comprehensive structural response of the complex geometry but present shakedown limit by adopting a conservative approach.

This research aims at analyzing shakedown and ratchet limit boundary of a 90° back-to-back pipe bends subjected to cyclic IP/OP bending and steady internal pressures by means of the LMM. Full cyclic incremental analysis known as step-by-step analysis is executed to verify the structural responses either side of each boundary. Parametric studies are carried out with respect to changes in geometry of the back-to-back pipe bend; semi-empirical equations are derived from relationships of the reverse plasticity limit and the limit pressure with the bend characteristic.

## NOMENCLATURE

$D_m$	Pipe bend mean diameter
$E$	Modulus of elasticity
EPP	Elastic perfectly plastic
$F_A$	Axial tension corresponding to PI
FEA	Finite Element Analysis
$h$	Bend characteristic of a pipe elbow
IP	In-plane
$L$	Vertical straight pipe length
LMM	Linear matching method
LP	Limit pressures
$M_L$	Moment to cause plastic collapse
NPS	Nominal pipe size
OP	Out-of-plane
$P_I$	Internal pressure to cause plastic collapse
$P_L$	Internal pressure considering $P_I$ and $F_A$
$R$	Pipe bend curvature
$r$	Pipe mean radius
$RP_{IP}$	Reverse plasticity limit under IP
$RP_{OP}$	Reverse plasticity limit under OP
RT	Ratio OP to IP
$t$	Pipe thickness
$\nu$	Poisson's ratio
$\sigma_y$	Yield stress of material

## STRUCTURAL RESPONSES UNDER CYCLIC LOADING

Under monotonic loading condition, a load level which a structure can withstand before plastic collapse is known “*limit load* “. For cyclic loading condition, a structure is likely to experience failures at lower load level. *Elastic limit*, *elastic shakedown*, *plastic shakedown*, and *ratchetting* are representative structural responses under such cyclic loading circumstances, graphically shown in Fig. 1.

The structure exhibits elastic response within the *elastic limit* throughout the cyclic loading. If the cyclic loading level increases over the yield stress, plastic strains begins to be accumulated, leading to following structural responses:

- *Elastic shakedown*: plastic strains are developed as producing constant residual stresses at initial loading, and then structural response shows entirely elastic.
- *Plastic shakedown*: plastic strains are developed under every loading cycle, but a closed loop is formed without increasing of net total strain range.

- *Ratchetting*: plastic strains are developed under every loading cycle, leading to an increment plastic collapse.

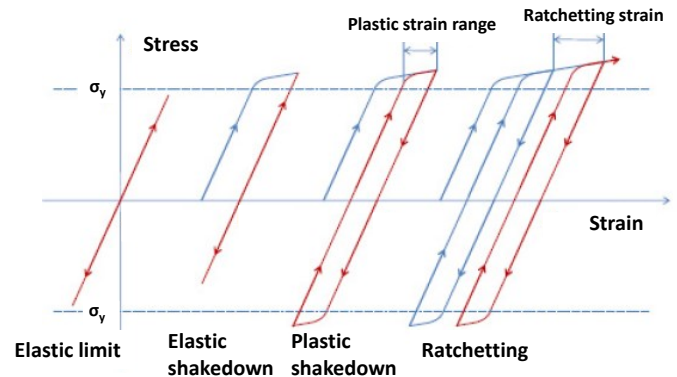


Fig. 1- Structural responses to cyclic loading condition.

For the general case, it allows a structure to experience up to elastic shakedown. Plastic shakedown response may also be permissible as long as the reverse plasticity does not affect structural integrity within a designed service life, throughout low cycle fatigue assessment. However ratchetting response is not accepted for a structure in the most case. If a structure is exposure to high temperature, creep rupture limit also should be taken into account as an important design limit.

## NUMERICAL METHOD

The LMM is a numerical analysis procedure following theoretical principals that represent nonlinear material responses using a series of linear elastic analyses where the elastic modulus at each integration point is allowed to be iteratively changed. This procedure repeats iteratively, which results in the redistribution of the stress level across a structure with the updated modulus, obtaining accurate upper and lower bounds to the shakedown and ratchet limits.

The LMM employs EPP model for the shakedown and ratchet analyses and is able to consider all possible loading scenarios. The LMM Abaqus subroutine has been adopted for assessment procedure for the high temperature response of structure in R5[14] based on its powerful performance. The LMM subroutines have been extended to evaluation of cyclic plasticity of structure considering full creep-fatigue interaction.

The numerical procedures to calculate shakedown and ratchet limit analysis have been introduced in extensive works[8, 9], therefore full numerical procedures of the LMM are not presented in this paper.

## FINITE ELEMENT MODEL

Fig. 2 shows geometry of the 90° back-to-back pipe bends with the two vertical pipe ends. In general pipe bends are expressed in terms of two ratios,  $R/r$  and  $r/t$ . The structure analyzed in this research is fabricated by bending a straight pipe. The pipe bend geometry refers to U.S. standard pipe size, which has 10 inches NPS Schedule 40. Pipe ovality/roundness is

not considered as the pipe bend is modelled with constant thickness. Dimensions of the geometry are listed in Table 1.

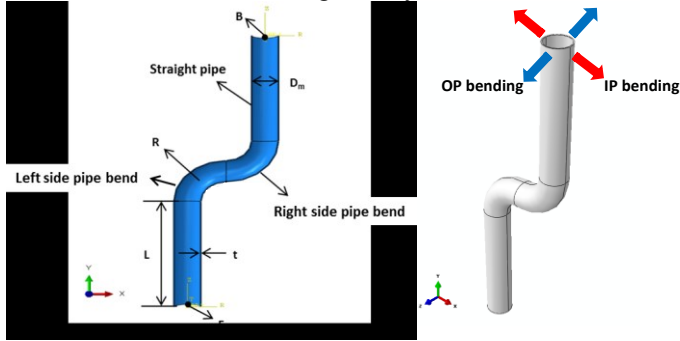


Fig. 2- Geometry of the 90° back-to-back pipe bends with two vertical pipes and IP(red) and OP(blue) bending mechanism.

Although the geometry is symmetric about x-y plane, full model of the pipe bends structure is created due to out-of-plane bending unable to apply for the half model. 3D solid element (C3D20R) is used to mesh the geometry for the analyses. Fig. 3 illustrates meshed pipe bends.

Table 1- Dimensions of the 90° back-to-back pipe bends and material properties.

$D_m$ [mm]	$t$ [mm]	$R(1.5NPS)$	$L=5D_m$ [mm]
263.78	9.27	381	1318.9
$E$ [GPa]	$\nu$	$\sigma_y$ [MPa]	
193.74	0.2642	271.93	

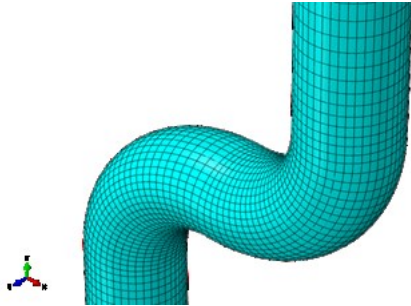


Fig. 3- 90° back-to-back pipe bends mesh.

Mechanical properties of material are the same as austenitic steel Type 304 LN[15] and listed in Table 1. This material is assumed to follow EPP behavior.

Two cylindrical coordinate systems are created at top and bottom of the vertical pipe and a reference node is created at the origin of each cylindrical coordinate as “B” and “F”. All nodes on the top and bottom surface of the vertical pipes are constrained to each corresponding reference node by kinematic coupling, while allowing the expansion/contraction in the radial direction.

Pattern of cyclic opening bending employed for the analyses is shown in Fig. 4 and steady internal pressure is also applied over the same period. To implement IP and OP bending moment, a clockwise moment about z axis and x axis on node “B” in Fig. 2 are applied respectively. Node “F” is fixed in all

degree of freedom. Internal pressure is applied to whole internal surface of the pipe bend structure. Axial tension is applied to all nodes on the top surface of the vertical pipe by considering closed end condition.

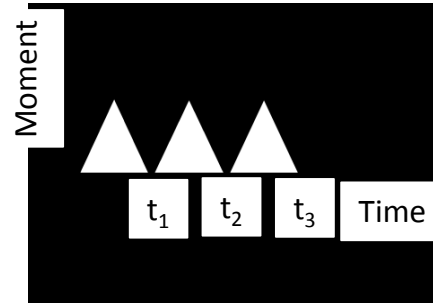


Fig. 4- Loading history of cyclic bending moment

Reference moment, pressure, and axial tension are calculated using Eqs.(1) to (3). These reference loads are used to normalize moment and pressure values computed by the LMM. The steady internal pressure and corresponding axial tension will be called as internal pressures  $P_L$  from now on.

$$M_L = \sigma_y D_m^2 t \quad (1)$$

$$P_L = \frac{2}{\sqrt{3}} (2\sigma_y t / D_m) \quad (2)$$

$$F_A = P_L D_m / 4t \quad (3)$$

The thin walled straight pipe having dimensions of the  $L$ ,  $D_m$ , and  $t$  is analyzed to construct limit load boundary using the LMM. The interaction curve is presented in Fig. 5, which satisfies the normalized limit moment and pressures for values of 1.0.

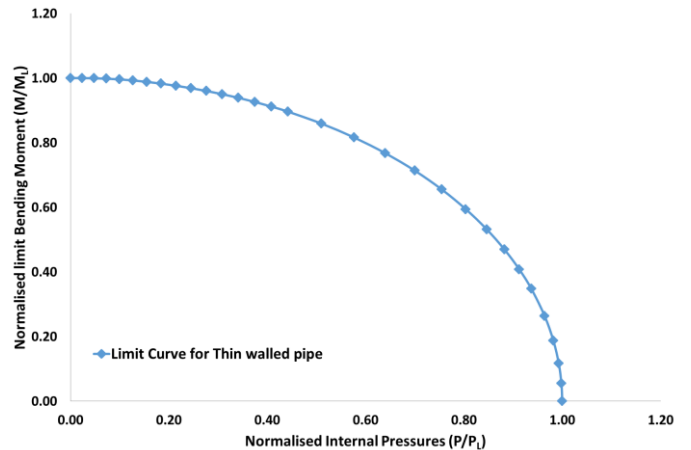


Fig. 5- Limit load boundary of the thin walled pipe bend under monotonic IP bending and steady internal pressure.

## NUMERICAL RESULTS

### IN-PLANE BENDING

To understand the back-to-back pipe bends' behavior, elastic analyses are performed under monotonic loading, which show that peak equivalent stresses are observed at right hand side flank for monotonic bending  $M_L$  and left hand side flank for monotonic bending  $P_L$  as Fig. 6. Shakedown and ratchet limit boundary are computed by the LMM and depicted in Fig. 7. Limit boundary of the back-to-back pipe bends indicates that the normalized limit moment and limit pressure decrease to 47% and 76% respectively, compared to the limit boundary of the thin walled straight pipe in Fig. 5. For the concerned pipe bend geometry, bending moment has severe impact on the integrity rather than internal pressure. A point to be noted is that peak normalized moment and pressure in Fig. 7 are not located on x and y axis, different from the limit boundary in Fig. 5. This is because that anticlockwise bending by  $P_L$  compensates the clockwise bending by  $M_L$  under the combined loading condition.

The shakedown limit boundary has similar form to a Bree-like diagram. The normalized cyclic moment at zero pressure is the reverse plasticity limit  $RP_{IP}$  where plastic strains begin to settle into a closed cycle, also known as "alternating plasticity". The normalized pressure at zero moment is the limit pressure where a structure will experience plastic collapse beyond this point.  $RP_{IP}$  is calculated as 36% of the straight pipe limit moment, which means low cycle fatigue assessment requires if designed cyclic bending exceeds this point. The constant  $RP_{IP}$  continues until  $P/P_L = 0.47$ , then decreases along with the shakedown boundary until  $P/P_L = 0.76$ .

The ratchet limit boundary is not the same as typical Bree-like diagram due to cyclic bending instead cyclic thermal loading. Thus the cyclic moment at zero pressure is intersected with the y axis. The ratchet boundary looks similar with the shakedown boundary for the concerned pipe bends. The normalized cyclic moment at zero pressure is identical to the limit moment of 47%, maintaining until  $P/P_L = 0.33$ . Afterwards it decreases and then converges to the shakedown boundary at  $P/P_L = 0.61$ . Areas between limit boundary and ratchet boundary are called "ratchetting zone" where plastic strain accumulates, leading to incremental plastic collapse.

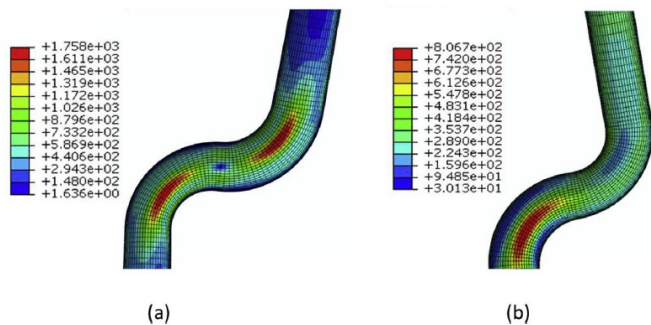


Fig. 6- Equivalent stress contours [MPa] from elastic solution under monotonic load; (a) IP bending  $M_L$  and (b)  $P_L$ .

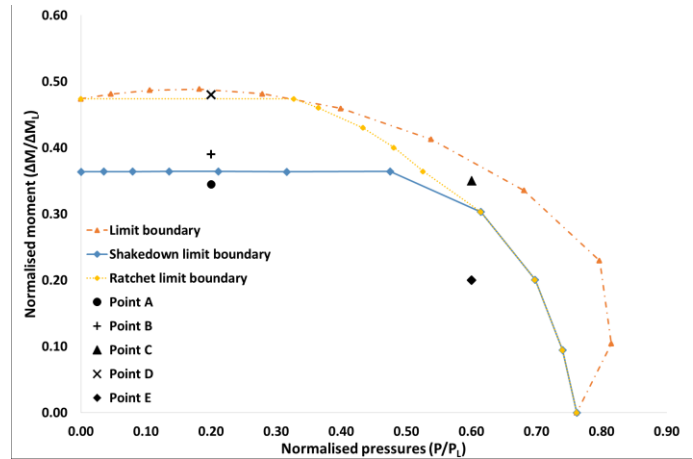


Fig. 7- Shakedown and ratchet limit boundary of the 90° back-to-back pipe bends under cyclic IP bending and steady internal pressure.

In order to verify the structural responses produced by the LMM, five individual cyclic loading points are created as labelled "A", "B", "C", "D", and "E". Full cyclic incremental analyses are performed to show plastic strain history for those five points, which are depicted by plotting plastic strain magnitude (PEMAG) over number of loading cycle in Fig. 8. The PEMAG considers sign of plastic strain in evolution, giving correct total plastic strain accumulation rather than Equivalent Plastic Strain (PEEQ). The plastic strain history of the all points is taken from the maximum PEMAG value among the eight Gaussian integration points.

The points A and E under the shakedown boundary clearly show the elastic shakedown mechanism with an initially accumulated plastic strain. The point B placed in between shakedown and ratchet boundary indicates the plastic shakedown mechanism by showing a constant plastic strain range. Finally the point C and D located in between ratchet boundary and limit boundary exhibit incremental plastic strain with every loading cycle. Although a margin where the point D belongs to is very small, the LMM can provide very accurate structural response.

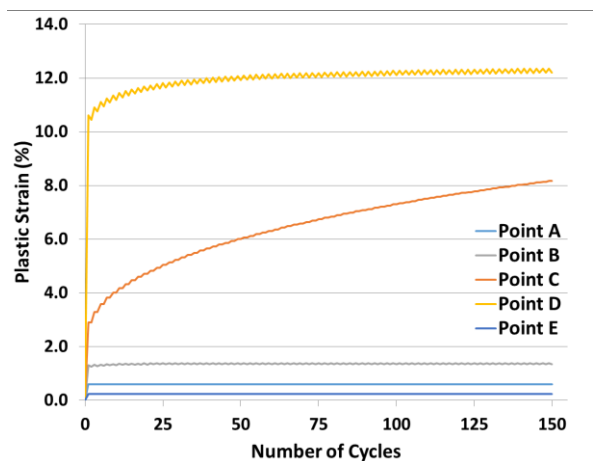


Fig. 8- Plastic strain magnitude for Points A, B, C, D, and E.

## OUT-OF-PLANE BENDING

Elastic stress analyses are performed under monotonic bending  $M_L$ , the peak equivalent stress occurs at front inner flank of left hand side pipe bend as shown in Fig. 9. Considering the symmetry of the pipe bend geometry in x-y plane, it is expected the peak stress level would occur at the opposite side, if anticlockwise monotonic OP bending was applied. Shakedown and ratchet limit boundary of the same pipe bends are presented in Fig. 10. Compared to the limit boundary in Fig. 5, the limit moment of the concerning pipe bends under the monotonic OP bending is 53%, but 6% higher than under monotonic IP bending. The limit pressure is the same as the one under monotonic IP bending due to identical geometry used for the analysis. Contrasting to the shape of limit boundary under monotonic IP bending, the peak limit moment and pressure under monotonic OP bending are smaller than the normalized limit loads on x and y axis, which means that the anticlockwise bending by  $P_L$  is not reduced during interaction of the both loadings.

The shakedown boundary under cyclic OP bending and steady  $P_L$  has very similar form to the limit boundary, unlike the shakedown boundary under IP bending in Fig. 7. The reverse plasticity limit  $RP_{OP}$  is very close to the limit moment. From  $P/P_y > 0.4$ , the margin between shakedown boundary and limit boundary starts to form until the limit pressure of 76%, but it is too narrow to determine the ratchet boundary. Therefore the ratchet boundary requires to be assumed to be same as the shakedown boundary in a conservative way. Consequently, enough margins under the shakedown boundary should be secured when designing allowable loading for the concerning pipe bends under cyclic OP bending and steady  $P_L$ .

Verification works are carried out to confirm the shakedown and ratchetting mechanism by plotting the plastic strain history over the number of loading steps as shown Fig. 11. The point A and B clearly indicate the elastic shakedown mechanism without further plastic strain increment at the steady state. The point C apparently shows the ratchetting mechanism with increment plastic strains within every cycle. Due to the small margin between the shakedown and limit load boundaries, the ratchetting limit boundary was difficult to be determined but the plastic strain history at point C confirms that the ratchet limit curve is very close to the shakedown limit boundary.

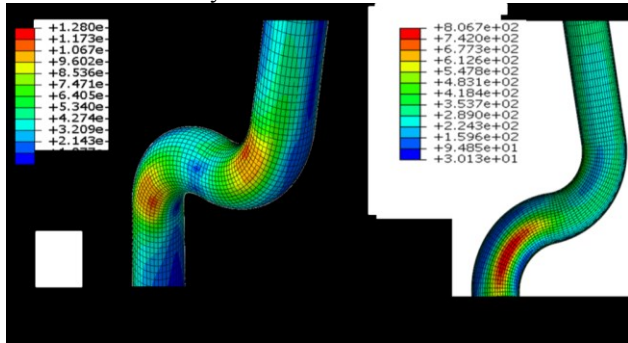


Fig. 9- Equivalent stress contours [MPa] from elastic solution under monotonic load; (a) OP bending  $M_L$  and (b)  $P_L$ .

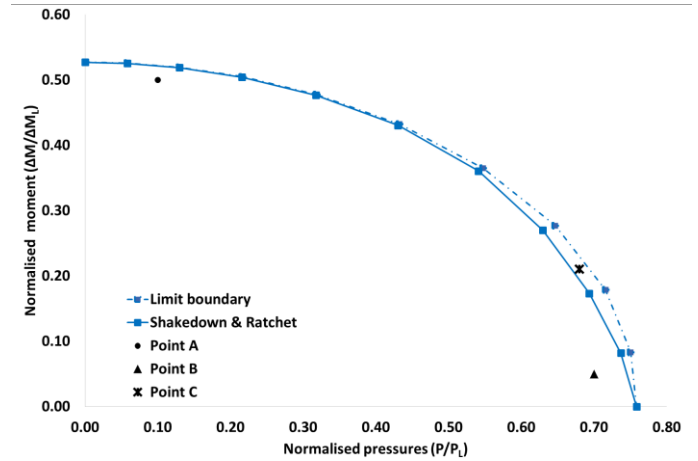


Fig. 10- Shakedown and ratchet limit boundary of 90° back-to-back pipe bends under cyclic OP bending and steady internal pressure.

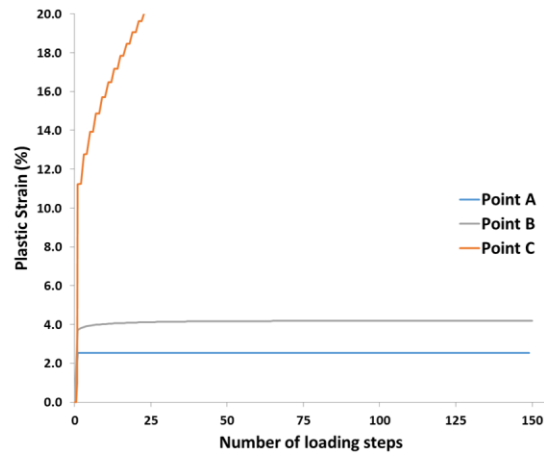


Fig. 11- Plastic strain history of points A, B, C.

## PARAMETRIC STUDIES AND DISCUSSIONS

Fig. 12 illustrates the varying geometries of 90° back-to-back pipe bends being used for the parametric studies. While  $r/t$  ratio is fixed, the effects of varying  $R/r$  ratio are observed.

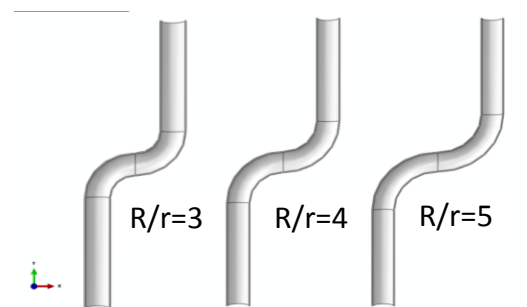


Fig. 12- Geometry in changes for the parametric studies.

Utilising the identical equations from (1) to (3), the reference cyclic bending and steady pressures for each  $r/t$  ratio are calculated as summarized in Table 2.

**Table 2- Reference loads with respect to r/t ratio.**

r/t	$M_L$ [Nmm]	$P_L$ [MPa]	$F_A$ [MPa]
5	4.991E+08	62.80	156.99
10	2.495E+08	31.40	156.99
20	1.248E+08	15.70	156.99

### IN-PLANE BENDING

Shakedown and ratchet limit boundaries for the fixed r/t ratio of 5, 10, 20 and varying R/r ratio 3, 4, 5 are presented in Fig. 13. The other geometries such as  $D_m$  and  $L$  are the same as dimensions in Table 1.

As general observations, reverse plasticity limit tends to decrease with an increase of r/t ratio, whereas limit pressure increases. As R/r ratio increase, reverse plasticity limit increases, but limit pressure decreases, unlike shakedown boundary of a single 90° elbow. Thus it should be considered that variation of the ratchet boundary of the back-to-back pipe bends with respect to R/r ratio is not identical to the single elbow.

For the thick walled pipe (r/t=5), shakedown boundaries equal to limit boundary until  $P/P_L < 0.3$ , leading to very small margin. Hence ratchet boundary should be considered as the shakedown boundary. An interesting point to be noted is that normalized pressure at R/r=5 becomes constant regardless normalized cyclic bending level less than 0.75. With decreasing R/r ratio, the trend of the normalized pressure appears with a decrease of the normalized cyclic bending level. However the variation of the normalized pressure is limited. Based on the observation, the thick walled back-to-back pipe bends are suitable application for higher cyclic bending to be expected during the operation.

For the thin walled pipes (r/t=10 and 20) shakedown boundaries have similar form to the Bree-like diagram. As R/r ratio increase, reverse plasticity limit increases but limit pressure decreases. The margin between shakedown and limit boundary tends to increase as R/r ratio decreases but as r/t ratio increases. For r/t=10, ratchet boundary at R/r=5 should be considered as shakedown boundary at the same R/r ratio. As R/r ratio decrease, reverse plasticity zone is clearly observed under the ratchet boundary. For r/t=20, ratchet boundaries are noticeable at every R/r ratio. On the basis of the findings, back-to-back pipe bends having r/t=10 are appropriate components at the operational loads where normalized cyclic bending and steady pressures are lower than 0.5. For the same pipe bends having r/t=20, it would be appropriate solutions for higher internal pressure to be expected due to lower endurance capacity against cyclic bending.

### OUT-OF-PLANE BENDING

Shakedown and ratchet limit boundary considering the same geometry effects as the previous study adopted are presented in Fig. 14.

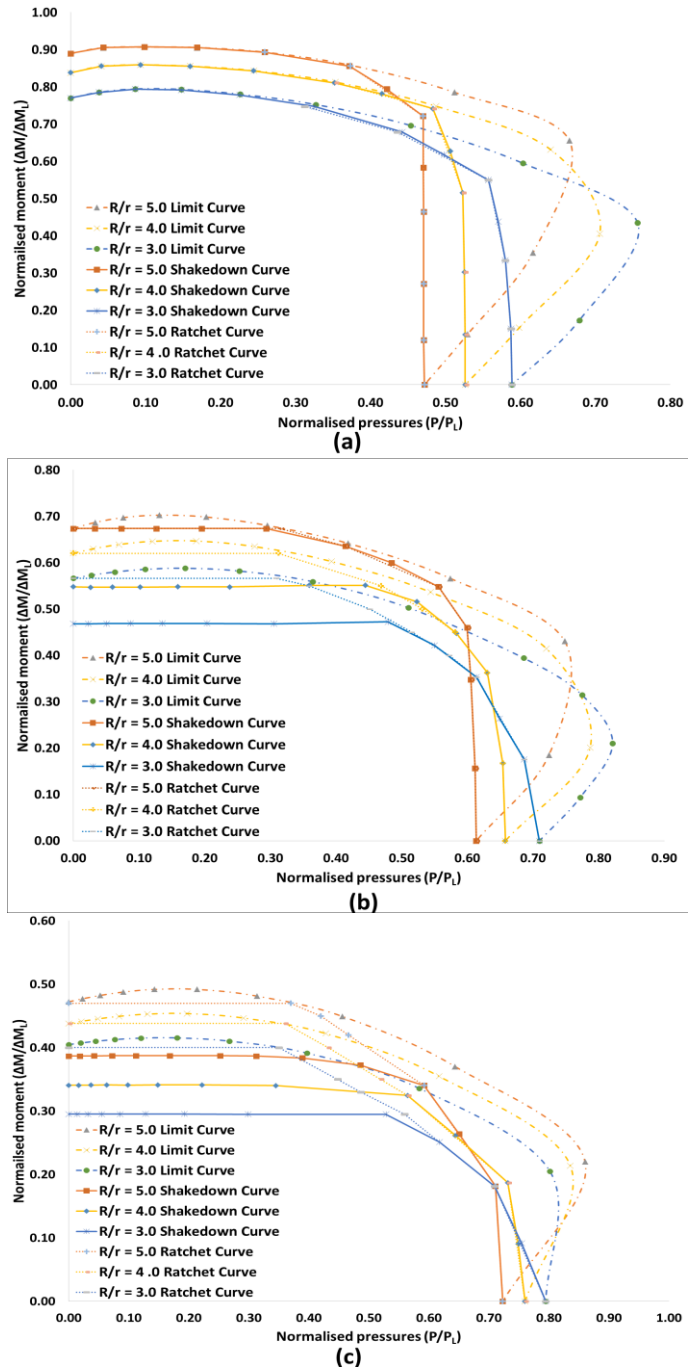


**Fig. 13- Effect of R/r ratio under cyclic IP bending and steady internal pressure; a) r/t =5, b) r/t=10, c) r/t=20.**

As general findings, the back-to-back pipe bends under cyclic OP bending and steady  $P_L$  shows that reverse plasticity limit decreases but limit pressure increases, with an increase of r/t ratio. As R/r ratio increases, reverse plasticity limit increase but limit pressure decrease. An interesting point to be noted is that shakedown boundary has a similar form to limit boundaries regardless the geometry effect, resulting in ratchet boundaries to be assumed as the shakedown boundaries. Hence, conservative

approaches should be used by selecting the operation loading underneath the elastic shakedown boundary, if the pipe bends are subjected dominant cyclic OP bending and steady  $P_L$ .

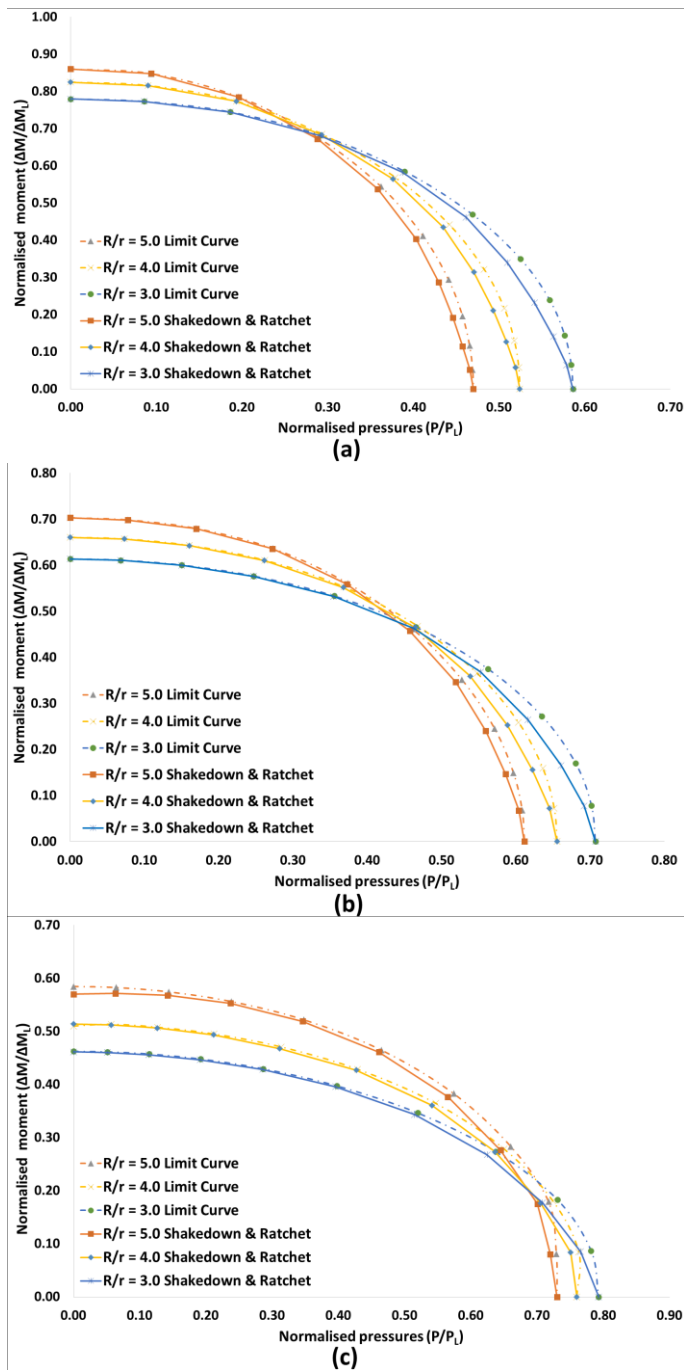


Fig. 14- Effect of R/r ratio under cyclic OP bending and steady internal pressure; a)  $r/t=5$ , b)  $r/t=10$ , c)  $r/t=20$ .

For the thick walled pipe ( $r/t=5$ ), shakedown boundaries are close to limit boundary at normalized pressures  $P/P_L < 0.3$ . The margin appears at  $P/P_L > 0.3$  but forms very small over the normalized pressure range. Although the margin becomes larger

with an increase of R/r ratio, it is too small to construct corresponding ratchet boundaries. In terms of the endurance capacity, the thick walled pipe bends have higher resistance to cyclic OP bending than steady  $P_L$ . The capacity increases at  $P/P_L < 0.3$  but turning in reduction at  $P/P_L > 0.3$ , with an increase of R/r ratio. Compared to  $RP_{IP}$  in Fig. 13 (a), the  $RP_{OP}$  have more or less the same values. However elastic shakedown zone under cyclic OP bending is smaller than under cyclic IP bending. Based on the observations, the thick walled pipe bends are suitable applications for high cyclic OP bending to be expected during the operation.

For the thin walled pipes ( $r/t=10$  and  $20$ ), shakedown boundaries have also similar forms to limit boundaries. The margin becomes smaller as  $r/t$  ratio increases, resulting in ratchet boundaries to be assumed as the shakedown boundaries. For  $r/t=10$ , both  $RP_{OP}$  and  $RP_{IP}$  are almost identical at  $R/t=5$ . As R/r ratio decreases,  $RP_{OP}$  is higher than  $RP_{IP}$ . Normalized pressure of 0.45 is the turning point for the endurance capacity to be in reduction with increasing of R/r ratio. For  $r/t=20$ , very small margin is reported at  $R/t=5$ , but the other shakedown boundaries are the same as corresponding limit boundaries. All  $RP_{OP}$  at  $r/t=20$  are higher than  $RP_{IP}$  at the same thickness, which means the same pipe bends can withstand larger magnitude of cyclic bending moment under OP direction rather than IP direction. The turning point is the normalized pressure of 0.68 at  $r/t=20$ . With those findings, it can be expected that the pipe bends having  $r/t=10$  are appropriate solutions for the normalized pressure higher than 0.6 during the operation. The thinnest walled pipe bends are likely suitable for the higher pressure cases.

Although the structural behaviors under cyclic loading are validated by the numerical analysis, it may require experimental validation of the numerical analysis as further works.

#### QUADRATIC RELATIONSHIPS

Quadratic relationships between  $RP_{IP}$  and the bend characteristic  $h$  are derived for a single pipe elbow [7]. Recently Cho and Chen introduced a correlation between  $RP_{IP}$  and LP with  $h$  for the same back-to-back pipe bends being used in this paper [16]. Utilizing the Quadratic Regression method, two quadratic equations between  $RP_{OP}$  and  $h$  and between RT and  $h$  are developed. The  $h$  can be expressed as Eq. (4). The calculated  $RP_{IP}$ ,  $RP_{OP}$ , LP, and RT values are summarized with respect to  $h$  in Table 3. The quadratic equations are defined as Eqs.(5) to (8), respectively. For the all presented equations have the R-squared value higher than 0.98.

Utilising these equations, piping system designer can predict approximated shakedown boundary of the back-to-back pipe bends with respect to varying geometry effects under both cyclic IP and OP bending and steady internal pressures without performing FEA.

**Table 3- Normalized reverse plasticity limit, limit pressure, and the ratio RT with respect to h.**

h	RP <sub>IP</sub>	RP <sub>OP</sub>	LP	RT
0.15	0.295	0.462	0.795	1.568
0.2	0.341	0.515	0.760	1.510
0.25	0.387	0.585	0.723	1.473
0.3	0.468	0.613	0.710	1.311
0.4	0.548	0.661	0.658	1.205
0.5	0.674	0.703	0.614	1.043
0.6	0.77	0.780	0.589	1.013
0.8	0.838	0.825	0.527	0.985
1	0.890	0.860	0.472	0.967

$$h = \frac{R/r}{r/t} = \frac{Rt}{r^2} \quad (4)$$

$$RP_{IP} = -0.784h^2 + 1.6242h + 0.0492 \quad (5)$$

$$RP_{OP} = -0.5032h^2 + 1.0227h + 0.3367 \quad (6)$$

$$LP = 0.2247h^2 - 0.6233h + 0.8751 \quad (7)$$

$$RT = 1.4312h^2 - 2.3624h + 1.9154 \quad (8)$$

## CONCLUSIONS

Shakedown and ratchet limit boundary are analyzed using the LMM for the 90° back-to-back pipe bends (10inches NPS Schedule 40 STD) subjected to cyclic IP and OP bending and steady internal pressure. Results presented in this paper show that cyclic bending gives more impact on the integrity of the concerning pipe bends than the internal pressure, particularly IP bending affects more than OP bending. The IP bending induces shakedown boundary which is typical shape of Bree-like diagram, as well as distinguishable corresponding ratchet boundary to be constructed within the margin between the shakedown and the limit boundary. However the OP bending results in shakedown boundary to be almost equal to corresponding limit boundary, so that resultant ratchet boundary should be assumed as the shakedown boundary. Although elastic shakedown boundary under OP bending is larger than under IP bending, conservative approach should be taken for the design of operational loading.

Parametric studies involving changes in geometry of the back-to-back pipe bends show following key remarks:

- Reverse plasticity limit tends to decrease with an increase of r/t ratio, whereas limit pressure increases.
- As R/r ratio increase, reverse plasticity limit increases, but limit pressure decreases, unlike shakedown boundary of a single 90° elbow.
- Under IP bending, as r/t ratio decreases, the margin becomes smaller at lower pressures  $P/P_L < 0.3$  so that

the conservative approach should be taken in order to avoid the plastic collapse.

- Under OP bending, the margin is very small regardless those effects of changes in geometry. Therefore ratchet boundaries should be taken into account as corresponding shakedown boundaries.
- Correlations of h with RP<sub>IP</sub>, RP<sub>OP</sub>, LP, and RT are shown in Eqs. (5) to (8) respectively, so that approximated shakedown boundary can be predicted without performing FEA.

Finally, this comprehensive numerical analysis delivers a good understanding of post yield behaviors of the popularly used pipe bends under cyclic loading. These results may be used to help the pipeline designer determine appropriate geometry for specific operating conditions. In addition, the analyzed results show a clear trend of the reverse plasticity limit, the limit pressure, and the shape of the boundaries with respect to the changes in the geometry and direction of cyclic loading.

## ACKNOWLEDGMENTS

The authors gratefully acknowledge the support of the University of Strathclyde during the course of this work.

## REFERENCES

1. Bree, J., *Elastic-plastic behaviour of thin tubes subjected to internal pressure and intermittent high-heat fluxes with application to fast-nuclear-reactor fuel elements*. The Journal of Strain Analysis for Engineering Design, 1967. **2**(3): p. 226-238.
2. Melan, E., *Theorie statisch unbestimmter Systeme aus ideal-plastischem Baustoff*. 1936: Hölder-Pichler-Tempsky in Komm.
3. Koiter, W.T., *General theorems for elastic-plastic solids*. 1960: North-Holland Amsterdam.
4. Mackenzie, D., J. Boyle, and R. Hamilton, *The elastic compensation method for limit and shakedown analysis: a review*. The Journal of Strain Analysis for Engineering Design, 2000. **35**(3): p. 171-188.
5. Seshadri, R., *Inelastic evaluation of mechanical and structural components using the generalized local stress strain method of analysis*. Nuclear Engineering and Design, 1995. **153**(2-3): p. 287-303.
6. Chen, H. and A.R. Ponter, *Shakedown and limit analyses for 3-D structures using the linear matching method*. International Journal of Pressure Vessels and Piping, 2001. **78**(6): p. 443-451.
7. Chen, H., et al., *Shakedown and limit analysis of 90 pipe bends under internal pressure, cyclic in-plane bending and cyclic thermal loading*. International Journal of Pressure Vessels and Piping, 2011. **88**(5): p. 213-222.

8. Giugliano, D., D. Barbera, and H. Chen, *Effect of fiber cross section geometry on cyclic plastic behavior of continuous fiber reinforced aluminum matrix composites*. *European Journal of Mechanics-A/Solids*, 2017. **61**: p. 35-46.
9. Zhu, X., et al., *Cyclic plasticity behaviors of steam turbine rotor subjected to cyclic thermal and mechanical loads*. *European Journal of Mechanics-A/Solids*, 2017. **66**: p. 243-255.
10. Chen, X., B. Gao, and G. Chen, *Ratcheting study of pressurized elbows subjected to reversed in-plane bending*. *Journal of Pressure Vessel Technology*, 2006. **128**(4): p. 525-532.
11. Oh, C.-S., Y.-J. Kim, and C.-Y. Park, *Shakedown limit loads for elbows under internal pressure and cyclic in-plane bending*. *International Journal of Pressure Vessels and Piping*, 2008. **85**(6): p. 394-405.
12. Abdalla, H.F., *Shakedown boundary determination of a 90° back-to-back pipe bend subjected to steady internal pressures and cyclic in-plane bending moments*. *International Journal of Pressure Vessels and Piping*, 2014. **116**: p. 1-9.
13. Abdalla, H.F. *Shakedown Boundary of a 90-Degree Back-to-Back Pipe Bend Subjected to Steady Internal Pressures and Cyclic Out-of-Plane Bending Moments*. in *ASME 2014 Pressure Vessels and Piping Conference*. 2014. American Society of Mechanical Engineers.
14. Ainsworth, R., *R5: Assessment procedure for the high temperature response of structures*. British energy generation Ltd, 2003. **3**.
15. Spindler, M., *ECCC Data Sheets 2014*. UK: ETD Ltd, 2014. **47**(2).
16. Cho, N.-K. and H. Chen, *Shakedown, ratchet, and limit analyses of 90° back-to-back pipe bends under cyclic in-plane opening bending and steady internal pressure*. *European Journal of Mechanics-A/Solids*, 2017.